Water Supply

Water Supply Vol 23 No 8, 3377 doi: 10.2166/ws.2023.170

Tunnel water burst disaster management engineering based on artificial intelligence technology – taking Yonglian Tunnel in Jiangxi Province as the object in China

Dandan Li[a], Haowen Xu[b,*], Ting Jiang[b], Hong Ding[b] and Yong Xiang[b]

[a] College of Materials and Environmental Engineering of Chengdu Technological University, Chengdu, Sichuan 611730, China
[b] School of Civil Engineering, Architecture, Environment, Xihua University, Chengdu, Sichuan 610039, China
*Corresponding author. E-mail: xuhaowen1@stu.xhu.edu.cn

ABSTRACT

Due to the influence of the groundwater system, mountain rock layers, climate rainfall, and tunnel length and depth, underground tunnels (UT) are prone to water inrush (WI) disasters, thus leading to delays and obstacles in construction projects. This paper takes the Yonglian Tunnel as the research objective and explores the water and mud inrush disasters that occurred from July to August 2012. The Yonglian Tunnel is a control project of the Jilian Expressway in Jiangxi Province. This paper aims to study and analyze the WI disaster management of the UT using artificial intelligence technology, and to deepen the understanding of its causes. It will affect the factors, hazards, and related disaster management engineering methods of the UT WI disaster. By establishing a back-propagation neural network model and a radial basis function neural network model, the risk of WI disasters in tunnels, the degree of harm caused by WI, and the ability to control them were predicted and analyzed, and the stability and error values of the models were compared.

Key words: artificial intelligence technology, disaster management engineering, tunnel engineering information, underground tunnel, water inrush

HIGHLIGHTS

- This paper aims to use artificial intelligence technology to study and analyze the water inrush disaster management of underground tunnels, and to deepen the understanding of its causes.
- Through the establishment of a back-propagation neural network model and radial basis function neural network model, this paper predicts and analyzes the risk of tunnel flood disaster, the degree of damage caused by flood and the control ability.

1. INTRODUCTION

In tunnel excavation engineering, water inrush (WI) accidents that occur due to inaccurate prediction of geological conditions in front of the tunnel face or overestimation of WI flow often result in casualties and significant economic losses for construction personnel. After the construction of the tunnel lining is completed, due to incomplete water inflow treatment, the lining leaks cause tunnel erosion damage. The corrosive leakage water has a more severe corrosion effect on the lining and tunnel auxiliary equipment. The repeated freeze–thaw cycles in cold regions cause frost heave and cracking of the lining concrete. In tunnel excavation engineering, WI accidents occur due to inaccurate prediction of geological conditions in front of the tunnel face or overestimation of the WI flow. Therefore, studying the key and difficult points of WI disaster management engineering in underground tunnels (UTs) can reduce the casualties and significant economic losses often caused for construction personnel.

The widespread distribution and rapid development of tunnel engineering construction have made the management of sudden flood disasters increasingly crucial and necessary. If an UT with the characteristics of a long tunnel line and buried depth happens to be built in a karst mountain or groundwater system vein area, the comprehensive impact would lead to frequent geological disasters of WI. In the process of managing WI disasters in UTs, various factors that may affect or cause WI disasters in tunnels need to be considered, including rock distribution, water system distribution, karst cave cracks, rainfall infiltration, building material characteristics, and so on. Based on the complexity of UT environmental WI disaster management engineering, the high-tech algorithms, machines, and technical analysis methods of artificial intelligence (AI) technology can be used to systematically and specifically analyze the key and difficult points of UT WI disaster management engineering while saving a lot of human and material resources (Almounajjed *et al.* 2023). This paper compares and verifies the differences between different analysis models established under AI technology, as well as the effectiveness of using them for WI disaster management in UT environments. This can help expand the research on WI management in the field of geological disasters and provide more innovative technical support for tunnel construction. Due to the susceptibility of UTs to WI disasters, based on AI technology, this paper studies the management engineering of environmental WI disasters in UTs, aiming to reduce delays and obstacles caused by WI disasters in construction projects. Also due to the susceptibility of UTs to WI disasters, based on AI technology, this paper studies the management engineering of environmental WI disasters in UTs, aiming to reduce delays and obstacles caused by WI disasters in construction projects. The conclusion is drawn that the back-propagation neural network (BPNN) model is more suitable for the application analysis of UT WI disaster management engineering (Xin *et al.* 2023; Yang *et al.* 2023).

In the process of controlling WI disasters in UT, research on the causes and solutions of disasters cannot be ignored, and targeted solutions such as rock seepage, pore pressure, mud impact, and WI from karst caves should be addressed. Xu Peng *et al.* conducted physical model tests to reproduce the water and mud inrush during the tunnel excavation process. After testing, it was found that the water and mud inrush process went through a seepage stage, high permeability flow stage, and attenuation stage. The changes in stage characteristics reflected the formation, development, and evolution of disasters (Xu *et al.* 2022). Wu *et al.* simulated the nonlinear WI process and studied the influence of the relative position of the tunnel surface and fault on the evolution of pore pressure and flow velocity near the tunnel surface (Wu *et al.* 2022). To study the hydraulic characteristics of fault rock in the process of water mud impact, D. Ma *et al*. described the momentum conservation of rock particle migration and three-phase fluid migration with an erosion constitutive formula and non-Darcy flow formula, and verified the accuracy of the proposed three-phase model (D. Ma *et al.* 2022). Li *et al.* established a new quantitative evaluation model based on reliability theory and genetic algorithm back-propagation neural network for predicting the consequences of WI disasters, which achieved effective results (Li *et al.* 2020). On the basis of research and analysis on a certain problem of WI in UT, it was also crucial to confirm the specific technical methods.

It is not rare that the fuzzy tomography, Bayesian network, random forest model, artificial neural network, and other methods of AI technology are applied to the study of WI and seepage in tunnels. Song *et al.* proposed a comprehensive method for the risk assessment of WI from faults in subsea tunnels by combining the intuitionistic fuzzy analytic hierarchy process and the Bayesian network. They also used sensitivity analysis technology to study various factors, which provided sufficient decision support for planners and engineers to prevent and control WI from tunnels (Song *et al.* 2021). Liu *et al.* believed that water seepage directly affected the operation safety of the tunnel and established a random forest seepage risk prediction model. After the case study, it was found that the sectional spalling area, crack width, and loss rate of the reinforcement section had a great impact on water seepage (Liu *et al.* 2021). Wen *et al.* established a WI risk analysis model based on the fuzzy Bayesian network on the basis of improving the risk definition. They established a multi-attribute group decision-making model according to the characteristics of tunnel WI risk control and determined the optimal WI risk management scheme (Wen *et al.* 2019). Yang *et al.* believed that cracks with high hydraulic conductivity were good waterways and WI channels in mines and tunnels. He analyzed the theory of using the back-propagation (BP) artificial neural network to predict the height of flow fault zones. By comparing the results with traditional calculations, it was found that the BP artificial neural network produced more reasonable results, which could be used to predict the height of water flow fracture zones (Yang *et al.* 2019). The aforementioned research process and achievements could serve as important references and a basis for the analysis and research of underground WI disaster management, thus providing a foundation and ideas for later researchers to conduct relevant research and applications.

The innovation of this paper is as follows: Compared with the traditional statistical analysis model, the neural network model has better persistence and timely predictability and can simultaneously solve the groundwater system prediction problem of multiple independent variables and dependent variables. Through Matlab simulation, the whole process of training and testing sample set construction, raw data preprocessing, neural network construction, training, testing, and evaluation results is studied.

2. UT ENVIRONMENTAL WI DISASTER MANAGEMENT PROJECT

2.1. Causes and influencing factors of WI in UTs

UT engineering mainly refers to tunnels built in underground rock layers and soil, generally including railways, highways, subways, and other tunnels. During tunnel excavation, WI may occur due to factors such as karst rock layers, groundwater veins, fissure seepage, construction errors, tunnel burial depth, and impact of rainfall and water accumulation (Wang *et al.* 2022). According to the different positions of WI in the tunnel, it can be divided into tunnel section WI, tunnel entrance WI, and tunnel surface WI. If it is based on the state of flowing water, it can be divided into dripping water, flowing water, curtain water, and stream water. It can be divided into karst cave fissure water, fault fissure water, and groundwater precipitation infiltration water based on the source of WI (S. Wang *et al.* 2020; Li *et al.* 2021). By analyzing the regularity of WI, it can be determined whether the WI in the UT belongs to sudden concentrated WI or a constant local WI. The causes and influencing factors of WI in UTs are shown in Figure 1.

The main factors affecting WI in UTs are geological conditions, groundwater, meteorological changes, and construction planning. The influence of geological conditions lies in the complex and special structure of rock formations and water veins in karst caves, karst areas, and water-rich areas. They are mainly divided into three types of geological conditions: fissure geology, karst geology, and harsh geology. The state patterns of WI under different geological conditions are different. There is no direct correlation between the three geological conditions. Generally, there are more karst caves and more complex rock formations in karst WI compared with the other two geological conditions. Therefore, karst WI problems occur more frequently and pose greater harm (Wang *et al.* 2019). The essence of tunnel WI disasters is the process of energy accumulation and explosion in the underground aquifer. Starting from the surrounding rock state of the aquifer structure and the height and direction of the groundwater level, UT WI can be processed (Cao *et al.* 2022). Based on the factors affecting WI in UT in Figure 1, after detailed analysis, the risk of WI disasters can be rated using the data obtained from the comprehensive judgment of each factor. Table 1 shows the risk assessment indicators for WI disasters in UT.

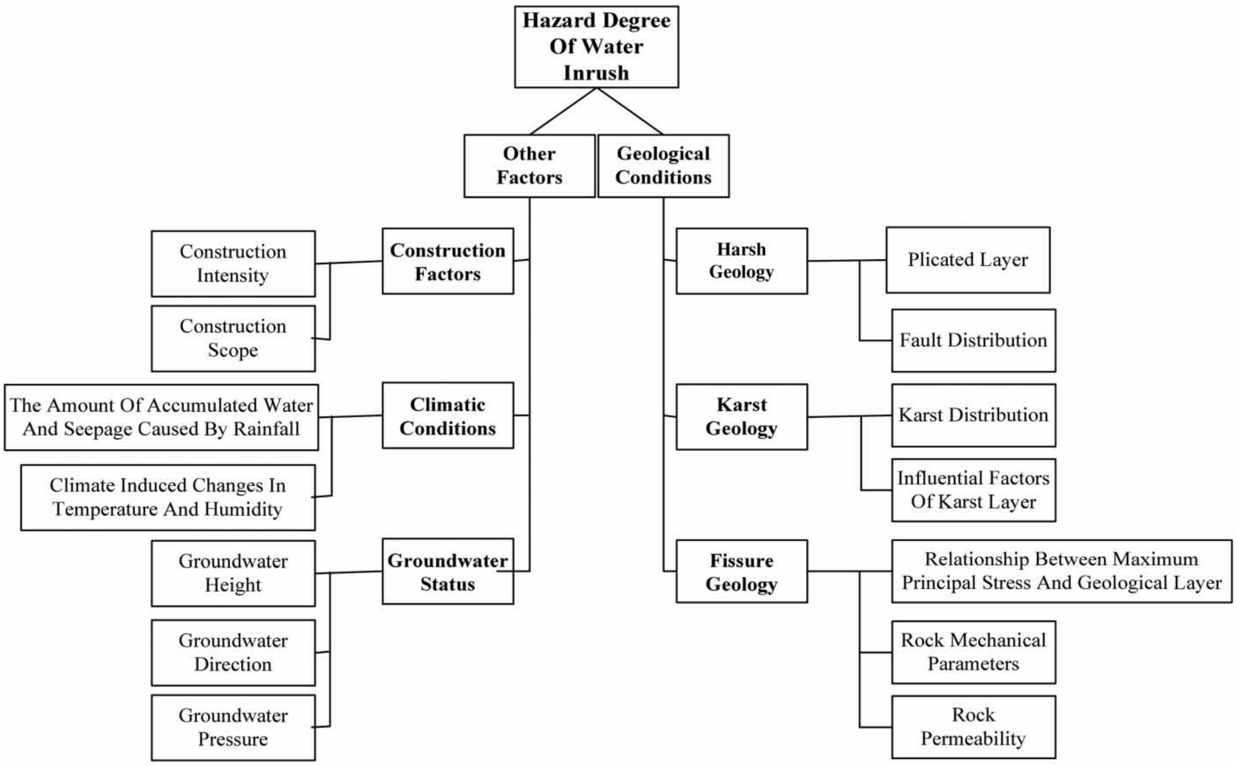

Figure 1 | Structural diagram of factors affecting WI in tunnels.

Table 1 | Risk assessment indicators for WI disasters in UT

Influencing factor indicators	Comprehensive evaluation		Risk rating	Risk level
7 Indicators related to geological factors	Determine whether each indicator is abnormal	Abnormal indicators 0–1	I	Scarcely possible
3 Indicators related to groundwater		Abnormal indicators 2–4	II	Tiny possibility
2 Indicators related to construction factors		Abnormal indicators 5–7	III	Highly possible
2 Indicators related to climate factors		Abnormal indicators 8–14	IV	Almost surely

2.2. WI disaster management project

At present, the treatment methods for WI disasters in tunnels are all based on four directions: prevention, drainage, interception, and interruption. The prevention measures should be analyzed separately from the situations of drainage, interception, and blocking before the occurrence of WI (Y. Ma *et al.* 2022).

The occurrence of WI in UT should be prevented. It is emphasized to take preventive measures in advance in construction planning, climate prediction, geological analysis, and various nodes of the tunnel where WI may occur. Among them, high-risk nodes in WI include tunnel shallow burial area, rock weathering area, near-surface water, karst layer development area, intersection and fusion area of different rock layers, and intersection area of the deep fracture zone (Hui *et al.* 2022).

The main preventive measures are as follows: During the tunnel route and the construction phase, high-risk areas are avoided in advance. According to the buried depth structure and geological conditions of the tunnel, corresponding drainage equipment is arranged and drainage design is strengthened; the monitoring and prediction of geological changes and climate precipitation are strengthened; the frequency and scope of monitoring and inspection at various nodes of the tunnel are increased (X. Wang *et al.* 2020). Under the premise of ensuring the prevention of WI in UT is in place, the probability and scale of WI can be greatly reduced, and the harm of WI can be reduced.

Under multiple preventive measures, after the occurrence of WI disasters, it is necessary to control the WI from the aspects of drainage, interception, and blocking. Common measures used to handle WI in tunnels include the use of advanced drilling equipment or auxiliary excavation of tunnels for drainage. Advance conduits can be used for pre-grouting to increase the soil adhesion of rock layers and block water inflow. This equipment is pre-used to fix rocks and rock formations and to inject mud to prevent water from gushing out. Light well points or deep pipe wells can be set up to drain accumulated water and lower the water level. Advance curtain grouting and tunnel expansion are used to seal the WI in the pilot tunnel (Fu *et al.* 2022; Li *et al.* 2022). The treatment of tunnels after water disasters is shown in Figure 2.

Figure 2 | Tunnel treatment after water disasters.

To analyze the treatment engineering of WI disasters in UT, in addition to obtaining data on the risk indicators of WI disasters in UT and rating the risks, it is also necessary to calculate and judge the unit time flow rate, velocity of flow, water pressure, area, degree of crack damage, rock mass strength, and other aspects of WI disasters to confirm the degree of harm of WI disasters and improve the efficiency of the related treatment work.

To estimate the amount of sudden water inflow, it is necessary to pour concrete grout stop walls on the excavation surface. After installing the drainage pipe, a water pressure gauge and flow meter need to be installed inside the pipe. According to the wall strength of the grout stop wall, the water outlet valve is closed in a timely manner, and the values on the water pressure gauge and flow meter are read every 15 min to obtain the approximate water inflow.

The relationship between the nozzle flow rate and pressure head can be used to estimate the height of surge head:

$$L = \frac{M^2}{2G\beta_x^2 D^2} \tag{1}$$

where L is the calculated head height; G is the gravitational acceleration of the water flow; D is the cross-sectional area of the nozzle; M is the water flow rate value at the nozzle; and β_x is the velocity coefficient of the water flow at the nozzle. The calculation of β_x is as follows:

$$\beta_x = \frac{1}{\sqrt{\gamma + \mu_x}} \tag{2}$$

where γ is the velocity distribution of the nozzle through the flow section measured by the flow meter, and μ_x is the local water loss coefficient of the nozzle flow.

The destructive nature of WI disasters in different UT environments varies. Karst geology and the occurrence of WI in areas filled with cracks can lead to the increase of cracks, and rock layers can move and collapse. The destructive evaluation formula for the hazards of WI in a fractured area is as follows:

$$s_\delta = \frac{1}{2}[s_1(1+\cos\alpha_0) - 3s_2\sin\alpha_0]\cos\frac{\alpha_0}{2} \tag{3}$$

In Equation (3), s_δ is the toughness value at which the material itself experiences fracture; s_1 is the stress intensity factor of water flow at one end of a tensile or torsional fracture occurring in a structural fracture; s_2 is the stress intensity factor of the water flow at the other end of the crack; and α_0 represents the angle at which the crack opens. Considering that most of the materials used for constructing UTs are concrete, the ultimate tensile strength of the concrete material itself when constructing tunnels and resisting WI and rock compression damage should be taken into account.

$$F = \varepsilon \frac{1.75\varphi t v}{\frac{6e}{v} - 1} \tag{4}$$

In Equation (4), ε is the longitudinal bending coefficient of the material; t is the width of the material interface; v is the thickness of the material cross-section; e is the cross-sectional compressive safety factor of the material; φ is the highest tensile strength value of concrete; and F is the ultimate bearing capacity of concrete under pressure within a certain area range and safety factor.

The treatment of WI in UTs cannot be separated from the drainage process. Drainage facilities can reduce accumulated water and discharge water during the prevention and treatment of sudden water surges. It can prevent the increase of water inflow and accumulation from damaging tunnel facilities. The rock pan can increase the drainage area and cut off the inflow of water, so as to provide convenience for grouting. The size of rock discs is affected by the amount of water discharged, the pressure value of the sudden water channel, and the external force value of the foundation at various parts of the tunnel. The formula is as follows:

$$K = \sqrt{\frac{15b(1-\vartheta^2)R^2}{40(f + \sum y_r V_r)}} \tag{5}$$

where K is the calculated rock disc size; b is the water pressure generated by the tunnel; ϑ represents the coefficient of Poisson's ratio of rock layers; R^2 represents the radius of the rock mass, where the rock plate is located; f represents the tensile strength of the rock mass, where the rock plate is located; y_r represents the thickness of underground rock layers; and V_r represents the weight value of underground rock layers.

3. APPLICATION OF AI TECHNOLOGY

AI technology is a computer science technology that needs to be used for research related to AI, involving machine learning, control and manufacturing of intelligent robots, computer vision, application of automatic programs, language translation and understanding, intelligent system manipulation, image recognition and generation, and so on (Reddy 2019). By using AI technology, computers can operate machines and programs more intelligently, thus achieving more flexible and autonomous functional operation. The analysis of the application of AI technology in the treatment of WI disasters in UTs requires analysis and decision-making on the factors that affect the treatment of WI disasters, the characteristics of WI disasters, and the treatment measures for different degrees of WI disasters. An AI technology model for the analysis of WI disaster treatment engineering in UT needs to be established (Daneshgaran *et al.* 2019).

The commonly used algorithms and technologies for building AI models include genetic algorithms, deep learning, artificial neural networks, annealing algorithms, maximum-minimum search algorithms, fuzzy logic, decision trees, and so on. These technologies are widely used for geotechnical risk assessment in tunnel engineering (Mikaeil *et al.* 2019; Tong & Wang 2021). Considering that artificial neural networks are more commonly used in the analysis of UT WI disaster management engineering, this paper used BPNN and radial basis function (RBF) neural networks in artificial neural networks to establish an engineering analysis model for UT WI disaster management.

3.1. Back-propagation neural network

The BPNN model is used to analyze and predict the risk and severity of WI disasters in UTs. The BPNN algorithm needs to be used to train and learn disaster evaluation index data such as geological conditions, climate factors, groundwater distribution area, rock structure, water flow, and water pressure of WI. The training and learning process is to forward transmit the input signal of the neural network and reverse transmit the error signal. The indicator information transmitted in the forward direction is transmitted from the input layer to the hidden layer until it enters the output layer. If the output layer result does not match the expected result, it is an error value. It is transmitted back to the input layer in the reverse direction. During the reverse transmission process, the weights of the neural connection points are corrected. After the corrected weight operation, the output error value will be smaller. By continually reducing the error value and training it, the prediction accuracy of the BPNN model is improved, and the efficiency of analyzing and predicting the risk and harm of WI disasters is greatly improved.

In a two-layer neural network, the input layer has x input values on the system, namely, $T^1, T^2, T^3, \ldots T^x$. These input values have y^1 elements: $F_1^1, F_2^1, F_3^1, \ldots F_{y^1}^1$. The right superscript 1 in this element represents the first layer of the neural network, and the right subscript represents the number of neurons in the first layer of the network. The input values and network layer representations of each element in the second and first layers are similar. The superscript 2 on the right of the element represents the second layer of the neural network, and the subscript on the right represents the number of neurons in the second layer of the network. The weights connected between x input values and y^1 elements are represented by β_{nk}^1. In this, k represents the connected neural network elements; n represents the input value; and the threshold of neural network elements is represented by a. The net value of the first input neuron is as follows:

$$S_1^1 = \sum_{n=1}^{x} \beta_{1n}^1 T^n + a_1^1 \tag{6}$$

By calculating the net value of the first input neuron, the value of S_k^1 is obtained. After function q^1, the output value of the first layer is obtained. Weight β_{dk}^2 is used for the connection between the first-layer network and the second-layer network. In this, d represents the neural elements of the second-layer network, and the net input values of the neural elements of the second-layer network are as follows:

$$S_d^2 = \sum_{k=1}^{y^1} \beta_{dk}^2 F_k^1 + a_d^2 \quad (d = 1, 2, 3, \cdots, y^2) \tag{7}$$

$$F_d^2 = q^2(S_d^2) \quad (d = 1, 2, 3, \cdots, y^2) \tag{8}$$

In the second-layer neural network, the output value of the neural network on the system is the final output of the second layer network and so on. Three-layer networks and even multilayer networks use a similar method to calculate the output value. The output values connected through all networks and neurons are transmitted forward or corrected in the event of errors, and finally, the output values of the entire BPNN are obtained. It is used to analyze and predict the risks and hazards of WI in tunnels, and the data of various indicators used for analysis and prediction in the network are input values and neural elements.

The specific algorithm flow is shown in Figure 3.

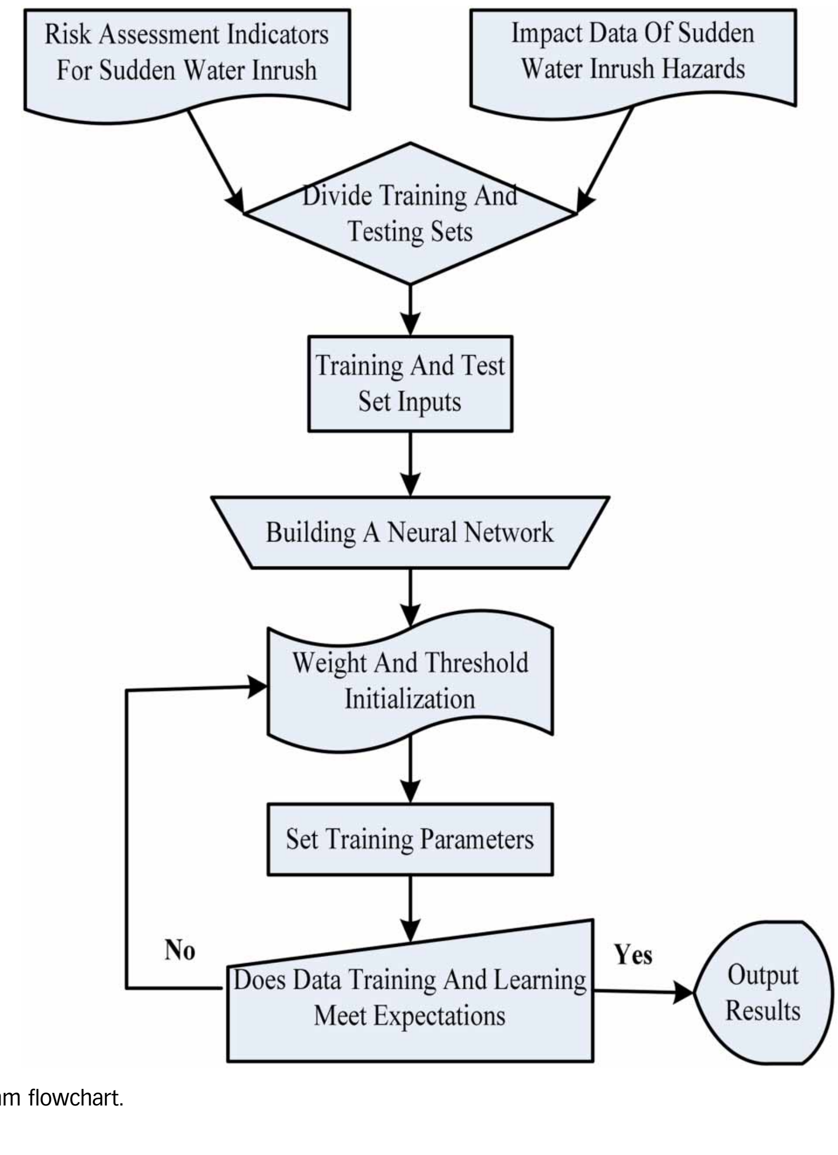

Figure 3 | BPNN algorithm flowchart.

3.2. RBF neural network

The radial basis function (RBF) neural network belongs to the feedforward neural network in artificial neural networks. The characteristic of the RBF neural network is its strong ability to classify data samples and overcome the minimum value of local data in the network, thus making the output results infinitely close to the expected accurate value. The neighboring layers in the network belong to unidirectional connections, which are different from those in BPNN with reverse transmission ability. The input layer and hidden layer belong to nonlinear transformations, while the hidden layer and output layer belong to linear transformations. The neurons in the hidden layer are connected and transmitted to the output layer through the RBF.

Let x represent the input element; y the ordinal number of hidden layer neurons; and S the output value. The RBF in the hidden layer can use the reflected sigmoid function, Gaussian function, or inverse multiquadric function. This paper used the Gaussian function as the RBF in the RBF neural network to construct the model. The number of hidden layer units in the network is represented by a and is expressed as follows:

$$\gamma_a B = \exp\left[-\frac{\|D - W_a\|}{2\varepsilon_a^2}\right]^2 \qquad (a = 1, 2, 3, \cdots, y) \tag{9}$$

In Equation (9), D represents the vector input at level x, and $D = [D_1, D_2, D_3, \cdots, D_x]^v$. W_a is the center vector of the ath hidden layer unit in the network. Due to the equal number of network layers between D and W_a, $W_a = [W_a^1, W_a^2, W_a^3, \cdots, W_a^x]$; $\|D - W_a\|$ is used as a norm to represent the radial distance between D and W_a; the maximum value of $\gamma_a B$ is above W_a and $\gamma_a B$ is inversely proportional to $\|D - W_a\|$; the width of the ath RBF in the neural network layer is represented by ε_a, and the width of the function is inversely proportional to the selectivity of the basis function. The hth output neural unit in the linear transformation unit from the hidden layer to the output layer is as follows:

$$U_h = \sum_{a=1}^{y} \beta_{ah} \gamma_a B \qquad (h = 1, 2, 3, \cdots, S) \tag{10}$$

In Equation (10), β_{ah} is the weight of the connection between the ath hidden layer and the hth output neural unit and U_h is the output value of the hth output neural unit. By evaluating the transformation from the input layer to the hidden layer and then to the output layer of the RBF neural network, the input tunnel WI risk index samples and hazard-related data samples can be obtained through model operation to obtain relevant predictive analysis results.

4. EXPERIMENTAL DATA EVALUATION

The Yonglian Tunnel is a control project of the Jilian Expressway in Jiangxi Province. The tunnel is designed as a bidirectional separated tunnel with a total length of 2.5 km. The left tunnel entrance is affected by the F2 fracture zone. From July to August 2012, there were eight water and mud inrush disasters, with an amount of about 1.7×10^4 m^3. From August to October 2012, there were seven water and mud inrush disasters in the right tunnel entrance, with a cumulative amount of about 2.3×10^4 m^3. After multiple water and mud bursts, a large-scale surface subsidence occurred on the mountaintop, with an area of about 2,000 m^2 and a depth of about 30 m. The complex geological conditions, large amount of mud outburst, frequent mud outburst, and high difficulty of treatment faced by the Yonglian Tunnel are rare in the world engineering community.

The WI disaster in the UT environment has a huge destructive effect on the construction and maintenance of the tunnel. The management of WI disasters is related to the smooth progress of the tunnel construction process. This paper would establish a model using the BPNN and RBF neural network, which have commonly been used for predicting and controlling tunnel WI disasters. This paper used data from WI risk assessment indicators to predict the risk of WI in tunnels. By using data related to the hazard level of WI, such as water inflow, fracture failure force, drainage facility efficiency, rock storage capacity, and tensile resistance of building materials, the accuracy of the model's analysis of the degree of harm caused by WI and its processing ability was judged. Finally, the paper also evaluated the stability and the error value of the model.

The experimental process is as follows: Classify governance plans to achieve targeted and strengthened governance; based on refined exploration results and analytic hierarchy process, select key holes for drainage and grouting; and in the classified and targeted grouting process, new grouting materials and process control technology are used to implement the treatment.

According to the real-time feedback information of surrounding rock deformation monitoring, the key parameters such as grout ratio and grouting pressure are dynamically adjusted to optimize the grouting design. At the same time, controllable drainage is realized through the key holes for drainage and grouting, and the water head pressure is reduced. After the treatment is completed, a comprehensive inspection method combining the drilling radar method, parameter analysis method, inspection hole method, and excavation sampling method is used to evaluate the grouting effect.

The map of the UT flood control geographic information system is shown in Figure 4. As shown in Figure 4, the data information used for model verification comes from websites such as TunnelNet, China Engineering Project Construction Network, and China Geographic Information Portal. By publishing data information on the website, this paper obtained and recorded information on 62 instances of completed tunnel engineering. It also conducted in-depth analysis of the length, burial depth, geological conditions of rock layers, climate and rainfall, construction planning, and construction technology of tunnel engineering. By substituting tunnel data with and without WI disasters into the model for verification and calculation, it was possible to compare the conditions for WI disasters in different tunnel environments. If all tunnel data that experienced WI disasters were selected, there would be a lack of data differences, which was not conducive to data analysis. The risk estimation and prevention data of WI disasters in the early stage of UT construction were compared and analyzed with the actual situation and hazard level data of WI disasters.

The time for disaster risk prediction using BP and RBF models is shown in Table 2. As shown in Table 2, when the number of iterations is 10, the risk prediction time of the BP neural network model is 2.23 s, and the risk prediction time of the RBF neural network model is 1.02 s; when the number of iterations is 30, the risk prediction time of the BP neural network model is 5.65 s, and the risk prediction time of the RBF neural network model is 2.66 s; when the number of iterations is 50, the risk prediction time of the BP neural network model is 12.33 s, and the risk prediction time of the RBF neural network model is 6.93 s.

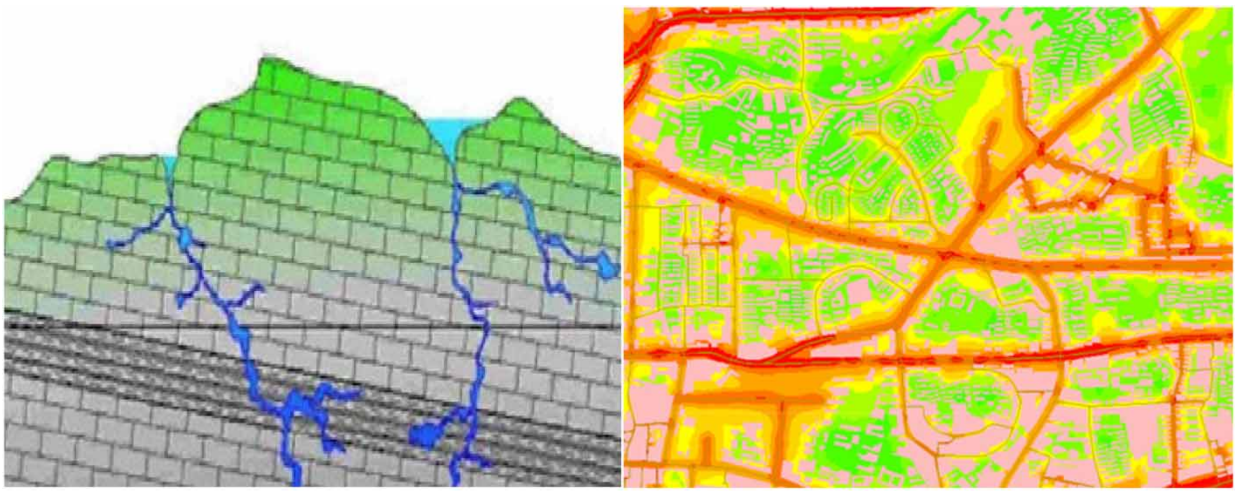

Figure 4 | Geographic Information System map of underground tunnel flood control.

Table 2 | Time for disaster risk prediction of BP and RBF models

Iterations	BP	RBF
10	2.23 s	1.02 s
20	4.98 s	1.81 s
30	5.65 s	2.66 s
40	8.51 s	4.37 s
50	12.33 s	6.93 s

The authenticity of disaster risk prediction using BP and RBF models is shown in Table 3. As shown in Table 3, when the number of iterations is 10, the authenticity of the BP neural network model risk prediction is 58.8%, and the authenticity of the RBF neural network model risk prediction is 98.7%; when the number of iterations is 30, the authenticity of the BP neural network model risk prediction is 60.6%, and the authenticity of the RBF neural network model risk prediction is 96.5%; and when the number of iterations is 50, the authenticity of the BP neural network model risk prediction is 63.2%, and the authenticity of the RBF neural network model risk prediction is 99.1%.

To fully test the performance advantages of the evaluation model and ensure the reliability of the data, this paper compared the experimental results of 50 iterations of the BPNN model and the RBF neural network model. Figure 5 shows the accuracy of the risk prediction of sudden WI disasters for the two models.

In Figure 5, the accuracy of the BPNN model in predicting the risk of WI in UTs was generally higher than that of the RBF neural network model. The highest accuracy of the BPNN model in predicting the risk of WI was 92.7% at the 31st time; the lowest prediction accuracy was 84.2% at the 37th time; the average prediction accuracy was 89.6%. The RBF neural network model was also used for risk prediction of WI in UTs. The highest accuracy rate was at the 47th time, accounting for 88.8%; the lowest prediction accuracy was at the fifth time, accounting for 81.4%; the average prediction accuracy was 85.3%.

This paper compares the accuracy of the two models in predicting WI risks in UT environments, which is a necessary task for conducting WI disaster management engineering analysis. In addition, it was also necessary to analyze and judge the degree of harm and handling capacity of WI disasters that occurred in the tunnel. Figure 6 shows the accuracy of the two models in analyzing the degree of harm and processing capacity of tunnel WI disasters that have occurred.

In Figure 6, the RBF neural network model had a significantly higher overall accuracy in analyzing the degree of harm and processing ability of WI disasters in UTs compared with the BPNN model. The BPNN model had its highest accuracy in

Table 3 | The authenticity of disaster risk prediction using BP and RBF models

Iterations	BP	RBF
10	58.8%	98.7%
20	62.1%	99.2%
30	60.6%	96.5%
40	59.3%	97.8%
50	63.2%	99.1%

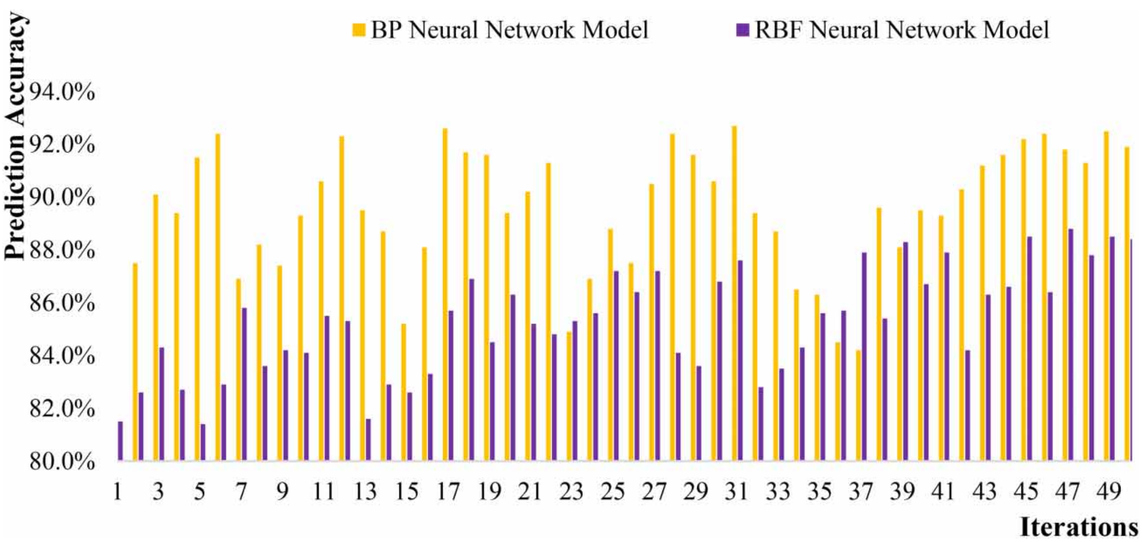

Figure 5 | Accuracy chart of disaster risk prediction for BPNN model and RBF neural network model.

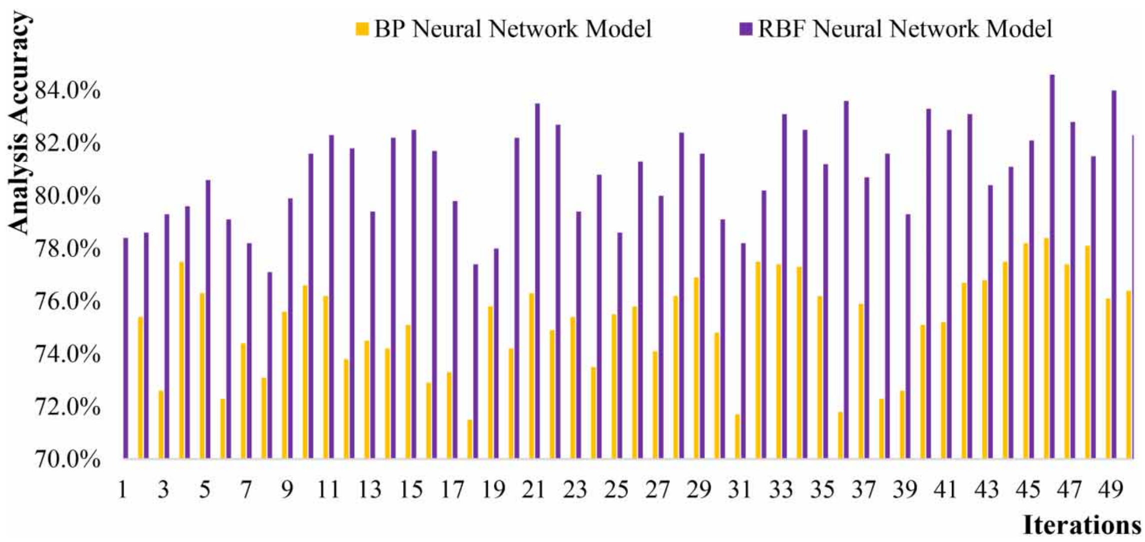

Figure 6 | Analysis accuracy of the degree of harm and treatment capacity of the two models in tunnel WI.

analyzing the degree of harm and processing ability of WI disasters when accounting for 78.4% in the 46th iteration experiment; the lowest analysis accuracy occurred in the 18th iteration experiment, accounting for 71.5%; and the average analysis accuracy was 75.2%. The RBF neural network had its highest accuracy in analyzing the degree of harm and processing ability of WI disasters in tunnels at the 46th time, accounting for 84.6%; the lowest was in the eighth round, accounting for 77.1%; and the average analysis accuracy was 80.9%.

After analyzing the risk, harmfulness, and resolution ability of WI in UTs using the two models, it was also necessary to evaluate the stability and error values of the models themselves. Figure 7 shows a comparison of the stability of the two models.

In Figure 7, by comparing the stability of the two models, it can be seen that the stability of the BPNN model showed an upward trend with the increase of iterations, while the stability of the RBF neural network model showed a downward trend with the increase of iterations. The stability changes of the BPNN model and the RBF neural network model intersect. The first half of the RBF neural network model had higher stability, while the second half of the BPNN model had higher stability.

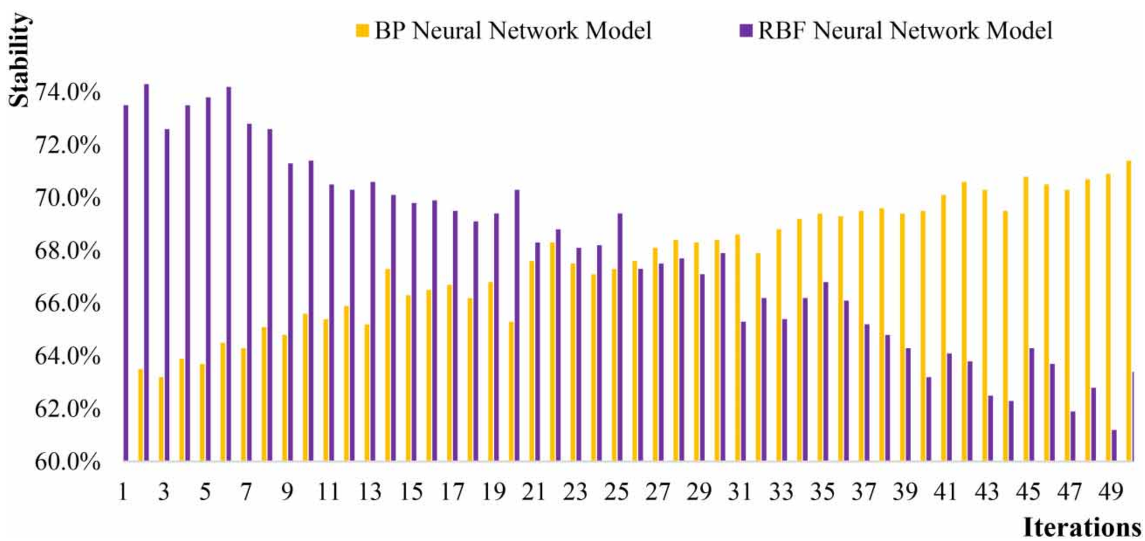

Figure 7 | Comparison of stability between the two models.

The stability of the BPNN model was the highest in the 50th iteration, accounting for 71.4%; the third iteration had the lowest stability, accounting for 63.2%; the average stability was 67.6%. The RBF neural network model had the highest stability in the second iteration, accounting for 74.3%; in the 49th iteration, the stability was the lowest, accounting for 61.2%; and the average stability was 67.9%. The average stability of the RBF neural network model was slightly higher than that of the BPNN model.

Figure 8 shows the comparison of error values between the two models. From Figure 8, it can be seen that with the 0-scale axis as the standard, the error values in the upper and lower positive and negative directions were smaller as they were closer to the 0-scale axis, and the error difference was larger as they were farther away from the 0-scale axis.

The error value of the BPNN model was generally smaller than that of the RBF network model, and the error value of the BPNN model generally decreased with the increase of iterations. The error value of the RBF neural network model increased with the number of iterations, and the fluctuation of the error value was more unstable. The maximum error value of the BPNN model was in the second iteration, which was −1.24; the minimum error value was 0.11 in the 48th iteration. The maximum error value of the RBF neural network model was at 32 times, which was −1.88; the minimum error value was at the 46th time, which was 0.22.

5. RESULTS AND DISCUSSION

5.1. The impact of BP neural network model on tunnel water disaster management

Tunnel WI has always been a major problem during tunnel construction. WI may cause delays in tunnel construction, cause huge property damage, and even lead to dangerous road collapses, resulting in casualties and mechanical damage. Based on the Yonglian Tunnel, the paper collected some data on the occurrence of WI during the construction process and used the BP neural network to predict the water inflow of the tunnel. In the actual prediction process of water inflow, it is necessary to combine the situation of the tunnel construction site and reasonably select influencing factors, so that the selected factors comprehensively reflect their impact on the tunnel water inflow, and there is no obvious correlation between them. Based on the geological conditions of tunnel engineering, the development of tunnel-surrounding rock fractures, the hydraulic conductivity of the surrounding rock fracture zone, the distance between the overlying bedrock fracture zone and the tunnel roof, the original water pressure of the overlying layer tunnel, and the depth of the tunnel are selected as the influencing factors of tunnel water inflow in this paper. The tunnel water inflow is predicted using a BP neural network, which consists of an input layer, a hidden layer, and an output layer. The neurons within the layer transmit information in a fully connected form, while there is no interconnection between each layer of neurons.

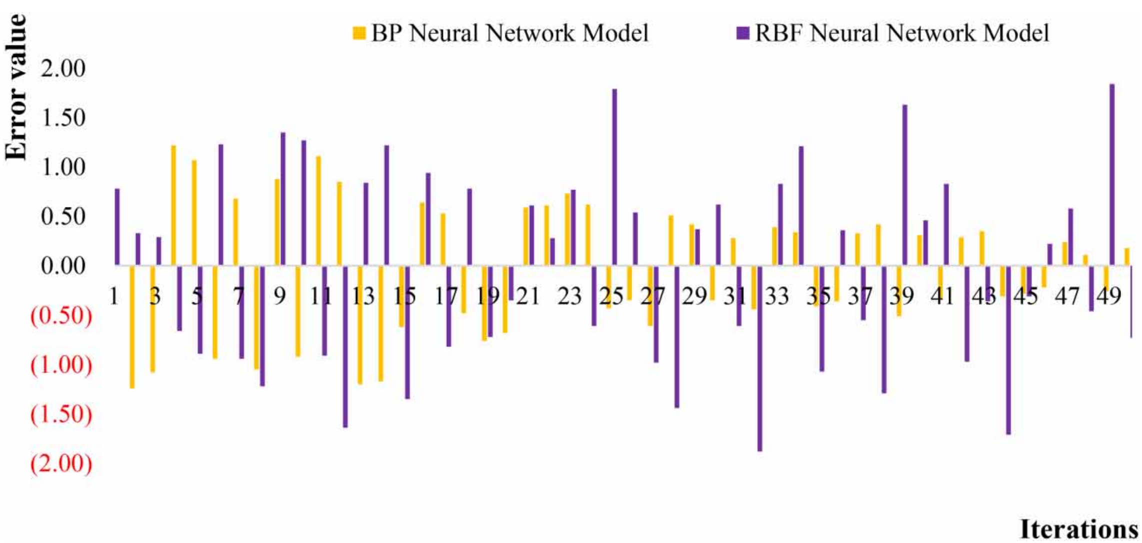

Figure 8 | Comparison of error values between the two models.

After obtaining training information from the sample tree data, the neural network activates the training information through neurons in the input layer. It passes information to hidden layer neurons through the processing of transfer functions and then transmits the final response result to the output layer through transfer function transformation. The output layer compares the training results with the expected output and feeds back information to each layer according to the principle of decreasing error. This allows each layer to continually adjust and correct the connection weights and thresholds between neurons based on the feedback of error information, until the training ends when the error meets the accuracy requirements. The convergence of this model is good, and there is a certain error between the predicted value and the actual value, but it is relatively small. The predicted results have a certain degree of reliability, providing a reference basis for the prediction method of tunnel water inflow.

5.2. Impact of RBF neural network model on tunnel water disaster management

RBF neural networks have excellent characteristics of structural adaptive determination and output independent of initial weights. Through Matlab simulation, this network was applied to the dynamic simulation and prediction of groundwater in a certain area, demonstrating the entire process of constructing training and detection sample sets, preprocessing raw data, training neural network construction, detection, and result evaluation. Good results were achieved, and compared with the BP network, the RBF network is a kind of a neural network model for groundwater dynamic simulation and prediction that is worth popularizing. The artificial neural network is a very effective means to deal with complex nonlinear problems. It has the characteristics of self-organization, self-learning, being adaptive, and so on. It is not only widely used in pattern recognition, image processing, nonlinear system identification, adaptive control, and other fields but is also widely used in dynamic prediction and optimal combination. Compared with traditional statistical analysis models, neural network models have better persistence and timely predictability and can be used to solve groundwater system prediction problems with multiple independent and dependent variables simultaneously. The RBF network has excellent characteristics of structural adaptive determination and output independent of initial weights. Through Matlab simulation, this paper studies the whole process of constructing training and detection sample sets, preprocessing original data, constructing the neural network, training, detection, and evaluation of results. The RBF network is a neural network model worth promoting for groundwater dynamic simulation and prediction. Currently, many people also use BP networks, which have shortcomings such as lower training speed and accuracy compared with RBF networks, as well as the impact of initial weights on results. At the same time, BP networks also have defects such as being prone to local minima during the learning process, being prone to oscillations, and having redundant connections or nodes in the network.

The problem of WI disasters during the construction and operation of UTs is extremely common, which can cause water accumulation, deformation, and safety hazards in the tunnel. This paper applied AI technology to the analysis of the treatment engineering of WI disasters in UTs. This mainly analyzed the reasons for the formation of WI, the relevant factors that affect the development of WI hazards, and various commonly used methods for treating WI disasters. By establishing a BPNN model and RBF neural network model through indicators, the predictive disaster risk ability of the two models applied to the analysis of WI disaster management engineering was analyzed, and the ability to solve WI hazards was analyzed through experimental demonstration. The advantages and disadvantages between the two models were evaluated.

6. CONCLUSIONS

This paper establishes the BPNN model and the RBF neural network in artificial neural networks under AI technology for the analysis of UT WI disaster management engineering. According to Figure 8, it can be seen that the comparison of error values between the two models shows that the maximum error value of the BPNN model appears in the second iteration, which is −1.24. In the 48th iteration, the minimum error value is 0.11. The maximum error value of the RBF neural network model is at 32 times, which is −1.88. The minimum error value occurrs at the 46th time, at 0.22. The following conclusion can be drawn: the error value of the BPNN model is usually smaller than that of the RBF network model, and as the number of iterations increases, the error value of the BPNN model usually decreases. The error value of the RBF neural network model increases with the number of iterations, and the fluctuation of the error value is more unstable. The RBF neural network model had a higher accuracy in analyzing the degree of harm caused by WI disasters and the processing ability of governance projects. Although the average stability of the model was slightly higher than that of the BPNN model, the difference was not significant. In view of the limited variety and quantity of applications and comparisons of AI technology in this paper, as well as the incomplete analysis of the influencing factors of WI disasters, there were certain limitations in the research content and conclusions, and there was room for further exploration.

DATA AVAILABILITY STATEMENT

All relevant data are included in the paper or its Supplementary Information.

CONFLICT OF INTEREST

The authors declare there is no conflict.

REFERENCES

Almounajjed, A., Sahoo, A. K., Kumar, M. K. & Subudhi, S. K. 2023 Stator fault diagnosis of induction motor based on discrete wavelet analysis and neural network technique. *Chinese Journal of Electrical Engineering* **9** (1), 142–157.

Cao, Z., Gu, Q., Huang, Z. & Fu, J. 2022 Risk assessment of fault water inrush during deep mining. *International Journal of Mining Science and Technology* **32** (2), 423–434.

Daneshgaran, F., Zacheo, L., Di Stasio, F. & Mondin, M. 2019 Use of deep learning for automatic detection of cracks in tunnels: prototype-2 developed in the 2017–2018 time period. *Transportation Research Record* **2673** (9), 44–50.

Fu, H., An, P., Cheng, G., Wen, S. & Li, J. 2022 Calculation of the allowable drainage of parallel tunnels based on ecological environment protection. *KSCE Journal of Civil Engineering* **26** (5), 2420–2427.

Hui, S., Sui, W., Zhang, G., Chen, J. & Yu, S. 2022 Plugging efficiency of pouring aggregates through multiple boreholes into an inundated tunnel to prevent groundwater inrush disasters. *Geoenvironmental Disasters* **9**, 15.

Li, Z., Wang, Y., Olgun, C. G., Yang, S., Jiao, Q. & Wang, M. 2020 Risk assessment of water inrush caused by karst cave in tunnels based on reliability and GA-BP neural network. *Geomatics, Natural Hazards and Risk* **11** (1), 1212–1232.

Li, S., Ma, C., Liu, R., Chen, M., Yan, J., Wang, Z., Duan, S. & Zhang, H. 2021 Super-absorbent swellable polymer as grouting material for treatment of karst water inrush. *International Journal of Mining Science and Technology* **31** (5), 753–763.

Li, Z., Chen, Z., He, C., Ma, C. & Duan, C. 2022 Seepage field distribution and water inflow laws of tunnels in water-rich regions. *Journal of Mountain Science* **19** (2), 591–605.

Liu, Y., Chen, H., Zhang, L. & Wang, X. 2021 Risk prediction and diagnosis of water seepage in operational shield tunnels based on random forest. *Journal of Civil Engineering and Management* **27** (7), 539–552.

Ma, D., Duan, H., Zhang, J., Liu, X. & Li, Z. 2022 Numerical simulation of water–silt inrush hazard of fault rock: a three-phase flow model. *Rock Mechanics and Rock Engineering* **55** (8), 5163–5182.

Ma, Y., Yang, J., Li, L. & Li, Y. 2022 Analysis on ultimate water pressure and treatment measures of tunnels operating in water rich areas based on water hazard investigation. *Alexandria Engineering Journal* **61** (8), 6581–6589.

Mikaeil, R., Haghshenas, S. S. & Sedaghati, Z. 2019 Geotechnical risk evaluation of tunneling projects using optimization techniques (case study: the second part of Emamzade Hashem tunnel). *Natural Hazards* **97** (3), 1099–1113.

Reddy, Y. R. 2019 An empirical study on the best prediction model of water inflow into drill and blast tunnels among several machine learning techniques. *International Journal of Emerging Technologies and Innovative Research* **6** (2), 888–891.

Song, Q., Xue, Y., Li, G., Su, M., Qiu, D., Kong, F. & Zhou, B. 2021 Using Bayesian network and intuitionistic fuzzy analytic hierarchy process to assess the risk of water inrush from fault in subsea tunnel. *Geomechanics and Engineering* **27** (6), 605–614.

Tong, D. & Wang, Y. 2021 Summary of application of fuzzy mathematics in construction project management. *World Journal of Engineering and Technology* **9** (3), 407–422.

Wang, Y., Chen, F., Yin, X. & Geng, F. 2019 Study on the risk assessment of water inrush in karst tunnels based on intuitionistic fuzzy theory. *Geomatics, Natural Hazards and Risk* **10** (1), 1070–1083.

Wang, S., Li, L., Cheng, S., Hu, H., Zhang, M. & Wen, T. 2020 Risk assessment of water inrush in tunnels based on attribute interval recognition theory. *Journal of Central South University* **27** (2), 517–530.

Wang, X., Lai, J., Qiu, J., Xu, W., Wang, L. & Luo, Y. 2020 Geohazards, reflection and challenges in mountain tunnel construction of China: a data collection from 2002 to 2018. *Geomatics, Natural Hazards and Risk* **11** (1), 766–785.

Wang, M., Wang, Y., Zhou, Z., Li, L., Deng, D. & Zhou, Q. 2022 Research on the evolution mechanism of water inrush in karst tunnel and the safety thickness of water-resisting rock mass. *Geotechnical and Geological Engineering* **40** (9), 4539–4549.

Wen, Z., Xia, Y., Ji, Y., Liu, Y., Xiong, Z. & Lu, H. 2019 Study on risk control of water inrush in tunnel construction period considering uncertainty. *Journal of Civil Engineering and Management* **25** (8), 757–772.

Wu, J., Wang, X., Wu, L., Lu, Y. & Han, Y. 2022 Parametric study of water inrush in a tunnel crossing a fault based on the 'Three Zones' fault structure. *KSCE Journal of Civil Engineering* **26** (8), 3600–3619.

Xin, Z., Zhang, J., Jin, Y., Zheng, J. & Liu, Q. 2023 Predicting the alloying element yield in a ladle furnace using principal component analysis and deep neural network. *Journal of Minerals, Metallurgy and Materials* **30** (2), 335–344.

Xu, P., Peng, P., Wei, R. & Zhang, Z. 2022 Model test of the mechanism underpinning water-and-mud inrush disasters during tunnel excavation in sandstone and slate interbedded Presinian strata. *Journal of Zhejiang University-Science A* **23** (11), 882–899.

Yang, L., Wen, X., Wu, X., Pei, L., Yue, C., Liu, B. & Guo, S. 2019 Height prediction of water flowing fractured zones based on BP artificial neural network. *Journal of Groundwater Science and Engineering* **7** (4), 354–359.

Yang, F., Xu, M., Lei, W. & Lv, J. 2023 Artificial intelligence methods applied to catalytic cracking processes. *Big Data Mining and Analytics* **6** (3), 361–380.

First received 28 April 2023; accepted in revised form 20 June 2023. Available online 12 July 2023